MAGNETIC RESONANCE IN CHEMISTRY
Magn. Reson. Chem. 2007; **45**: 962–970
Published online in Wiley InterScience
(www.interscience.wiley.com) DOI: 10.1002/mrc.2086

MRC

Solid state NMR characterization of individual compounds and solid solutions formed in Sc_2O_3–V_2O_5–Nb_2O_5–Ta_2O_5 system

Dzhalil Khabibulin,[1] Konstantin Romanenko,[1] Mikhail Zuev[2] and Olga Lapina[1]*

[1] Boreskov Institute of Catalysis, SB RAS, Prosp. Lavrentieva 5, 630090 Novosibirsk, Russia
[2] Institute of Solid State Chemistry, UB RAS, 620219 Ekaterinburg, Russia

Received 1 May 2007; Revised 22 June 2007; Accepted 20 August 2007

In this study, ^{51}V, ^{45}Sc and ^{93}Nb MAS NMR combined with satellite transition spectroscopy analysis were used to characterize the complex solid mixtures: $VNb_{9(1-x)}Ta_{9x}O_{25}$, $ScNb_{(1-x)}Ta_xO_4$ and $ScNb_{2(1-x)}Ta_{2x}VO_9$ (x = 0, 0.3, 0.5, 0.7, 1.0). This led us to describe the structures of Sc and V sites. The conclusions were based on accurate values for ^{51}V quadrupole coupling and chemical shift tensors obtained with ^{51}V MAS NMR/SATRAS for VNb_9O_{25}, VTa_9O_{25} and $ScVO_4$. The ^{45}Sc NMR parameters have been obtained for Sc_2O_3, $ScVO_4$, $ScNbO_4$ and $ScTaO_4$. On the basis of ^{45}Sc NMR and data available from literature, the ranges of the ^{45}Sc chemical shift have been established for ScO_6 and ScO_8. The gradual change of the ^{45}Sc and ^{51}V NMR parameters with x confirms the formation of solid solutions in the process of synthesis of $VNb_{9(1-x)}Ta_{9x}O_{25}$ and $ScNb_{(1-x)}Ta_xO_4$, in contrast to $ScNb_{2(1-x)}Ta_{2x}VO_9$. The cation sublattice of $ScNb_{(1-x)}Ta_xO_4$ is found to be in octahedral coordination. The V sites in $VNb_{9(1-x)}Ta_{9x}O_{25}$ are present in the form of slightly distorted tetrahedra. The ^{93}Nb NMR parameters have been obtained for VNb_9O_{25}. Copyright © 2007 John Wiley & Sons, Ltd.

KEYWORDS: solid state NMR; SATRAS; MAS; ^{51}V; ^{45}Sc; ^{93}Nb; solid solutions; bulk oxides; vanadates; niobates

INTRODUCTION

The solid solutions based on vanadates of rare-earth elements (REE) are used as photo-, cathodic-, X-ray-luminophors, ceramics with a huge dielectric constant, as X-ray contrast agents in medicine and in other applications.[1–5] The complex mixed vanadia-based (V-Nb-Ta-O) oxides are used as oxide catalysts for various processes.[6,7] An active phase of these complex catalysts can be found in a form of corresponding solid solutions. The properties and applicability of solid solutions significantly depend on their composition and structure and present significant interest. The detailed structural characterization is an essential step for the improvement of synthesis methods.

The structural and other properties of solid solutions formed in M_2O_3–V_2O_5–R_2O_5 systems (M = REE, R = Nb, Ta) depend on REE. For example, two series of solid solutions were found in MVO_4–Nb_2O_5–Ta_2O_5 (M = La, Y):[8,9] $MTa_{2(1-x)}Nb_{2x}$ VO_9 (x = 0–0.1 for La, and x = 0–0.09 for Y) and $MNb_{2(1-x)}Ta_{2x}$ VO_9 (x = 0–0.4 for La, and x = 0–0.58 for Y). A continuous series of solid solutions $VNb_{9(1-x)}Ta_{9x}O_{25}$, $ScNb_{1-x}Ta_xO_4$ and $ScTa_{2(1-x)}Nb_{2x}$ VO_9 (x = 0–1) were found in Sc_2O_3–V_2O_5–Nb_2O_5–Ta_2O_5.[5,10] The replacement of atoms in the anion and cation sublattices during the formation of solid solutions needs a detailed consideration. It is known that vanadium tends to change its charge in such compounds. Therefore, since the samples are synthesized under air atmosphere a part of V^{5+} ions was reduced to V^{4+}. Investigation of V^{4+} defects in $ScNb_{2(1-x)}Ta_{2x}$ VO_9 have been performed by Zolotukhina *et al*.[5]

Solid state NMR of quadrupolar nuclei provides us with detailed structural information on a number of nonequivalent sites, coordination numbers, coordination sphere distortion and association of polyhedra. Advantages of solid state NMR spectroscopy over the diffraction techniques permit probing of both the crystalline and highly amorphous phases providing the unique insight into structure and disorder of solids.[11] Anisotropic interactions of quadrupolar nuclei broaden the powder spectra, thus complicating the data analysis. Among the multiple techniques which improve the spectral resolution and facilitate the spectral analysis, the most useful ones are: ultra-high speed magic angle spinning (UH MAS), multi-quantum magic angle spinning (MQ MAS), satellite transition spectroscopy (SATRAS), and STMAS.

In addition to the extensively explored solid state ^{51}V NMR[12,13] the increasing interest to solid state ^{45}Sc[14–21] and ^{93}Nb[16,22–30] NMR is indicated. The ^{51}V ($I = 7/2$), ^{45}Sc ($I = 7/2$) and ^{93}Nb ($I = 9/2$) are relatively sensitive quadrupolar nuclei (0.38, 0.3 and 0.482 relative to ^{1}H, respectively) with acceptably large quadrupolar moments (-0.0515×10^{-28}, -0.22×10^{-28} and -0.28×10^{-28} m^2, respectively).

In this study the systematic characterization of the structural changes of complex solid mixtures $VNb_{9(1-x)}Ta_{9x}O_{25}$,

*Correspondence to: Olga Lapina, Boreskov Institute of Catalysis, SB RAS, pr. Lavrentieva, 5, 630090 Novosibirsk, Russia.
E-mail: olga@catalysis.ru

$ScNb_{(1-x)}Ta_xO_4$, and $ScNb_{2(1-x)}Ta_{2x}VO_9$ ($x = 0.$ 0.3, 0.5, 0.7, 1.0) related to the substitution effects (replacement of Nb^{5+} to Ta^{5+}) was performed using ^{51}V, ^{45}Sc and ^{93}Nb MAS NMR followed by satellite transition analysis.[31–33] Analysis of the manifold of spinning sidebands allowed us to determine the parameters of quadrupole (C_Q, η_Q) and chemical shift (δ_{CS}, η_{CS}, δ_{iso}) tensors. In addition, the ^{93}Nb NMR parameters were measured using high magnetic field.

EXPERIMENTAL

The main part of the measurements was performed using Bruker MSL-400 (9.4 T) spectrometer at resonance frequencies 105.20, 97.17 and 97.77 MHz for ^{51}V, ^{45}Sc and ^{93}Nb, respectively. Bruker 4.0 and 2.5 mm MAS probes and 5 mm MAS probe from NMR Rotor Consult ApS (Denmark) were used for acquisition of static and 15–35 kHz MAS spectra. High field facility (19T) was used in ^{93}Nb NMR experiments. The single pulse sequence with rf-pulse duration of 1 μs (less then $\pi/10$) and recycling time from 0.1 to 5 s for all nuclei was used. The static ^{51}V spectra were acquired using Quad-Echo pulse sequence $90x$-τ-$180y$-τ with τ varying from 50 to 200 μs.

The ^{45}Sc, ^{93}Nb and ^{51}V chemical shifts were referred to 0.01 M solution of $ScCl_3$ in water, saturated solution of $NbCl_5$ in wet acetonitrile and $VOCl_3$, respectively. The computation of static and MAS ^{51}V NMR spectra was performed using NMR5 software[34–36] on a dual PII-400 MHz CPU IBM PC compatible computer running on Linux OS. The ^{45}Sc NMR parameters were obtained by analysis of static and MAS spectra by the method described in. Ref. 36 The relative orientations of EFG and CSA tensors: angles are proposed only for Sc. The parameters were analyzed for both static and MAS spectra.

The samples were synthesized by multi-stage annealing of initial components (Sc_2O_3, Ta_2O_5, Nb_2O_5 and V_2O_5) mixtures in air.[5] The purity of the initial components was 99.99%. These components were mixed considering the stoichiometry and ground in agate mortar under ethyl alcohol. The powders were sintered in corundum boats at temperatures between 600 and 1100 ± 25 °C. The x-ray analysis of the samples was carried out at room temperature using DRON-20 diffractometer (CuKα-radiation). X-ray analysis of the individual compounds ($ScVO_4$, $ScNbO_4$, $ScTaO_4$, VNb_9O_{25}, and VTa_9O_{25}) did not confirm the presence of impurities. According to ^{51}V NMR, content of impurities does not exceed 0.5%. A continuous series of solid solutions $ScNb_{(1-x)}Ta_xO_4$, $VNb_{9(1-x)}Ta_{9x}O_{25}$, $ScNb_{2(1-x)}Ta_{2x}VO_9$ ($x =$ 0–1) was reported to exist in the Sc_2O_3–V_2O_5–Nb_2O_5–Ta_2O_5 system, Fig. 1.[5,10] All phases are crystalline: $VNb_{9(1-x)}Ta_{9x}O_{25}$ and $ScNb_{2(1-x)}Ta_{2x}VO_9$ are isostructural to VNb_9O_{25}, and $ScNb_{(1-x)}Ta_xO_4$ is isostructural to $Fe(WO_4)$.[10]

RESULTS AND DISCUSSION

Correct analysis of ^{51}V, ^{45}Sc, and ^{93}Nb NMR spectra of solid solutions requires the NMR 'fingerprints' of the 'suspect' individual compounds found with the phase relations. These individual compounds are: V_2O_5, VNb_9O_{25}, VTa_9O_{25}, $NbVO_5$, $TaVO_5$, $NbTaV_2O_{10}$, $ScVO_4$, $ScNb_2VO_9$ and $ScTa_2VO_9$, Sc_2O_3, $ScNbO_4$, $ScTaO_4$ and Nb_2O_5 (see Fig. 1 with the corresponding phase relations from Ref. 10).

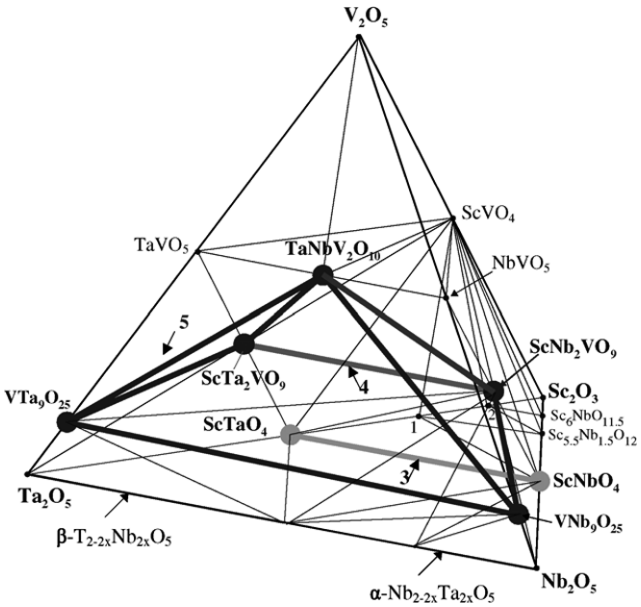

Figure 1. Subsolidus phase relations of Sc_2O_3–V_2O_5–Nb_2O_5–Ta_2O_5: (1) Sc_3TaO_7, (2) $Sc_6TaO_{11.5}$, (3) $ScNb_{(1-x)}Ta_xO_4$, (4) $ScNb_{2(1-x)}Ta_{2x}VO_9$, (5) the region of the VNb_9O_{25} based solid solutions, Ref. 10.

Several types of vanadium sites can be distinguished from ^{51}V chemical shift and quadrupole tensor parameters obtained with SATRAS.[13] Tetrahedral vanadium sites denoted by Q^0, Q^1, and Q^2 are apparent from the correlation between the type (η_{CS}–chemical shift asymmetry parameter) and value (δ_{CS}–chemical shift anisotropy–CSA) of the chemical shift tensor. Nonequivalent vanadium sites can be distinguished using a correlation between *effective* $\delta_\perp$ estimated as $\delta_\perp = 1/2(\delta_1 + \delta_2)$, δ_i- components of CS-tensor, and quadrupolar coupling constant (C_Q).

A C_Q range known so far for Sc is 10–25 MHz. The ranges of chemical shift are approximately 250 for solutions[37] and 200 ppm for oxide systems.[19–21] The isotropic chemical shift of ^{93}Nb is sensitive to oxygen coordination number (NbO_x): for four-coordinated Nb sites the isotropic shift ranges from −650 to −950 ppm; for five-coordinated Nb sites the range is rather narrow −900 to −980 ppm; six-coordinated Nb – from −900 to −1360 ppm; seven-coordinated Nb from −1200 to −1600 ppm; eight-coordinated Nb appears in the fields higher than −1400 ppm.[30] Thus, the ^{93}Nb chemical shift varies in the range from −650 to −1600 ppm. The Nb quadrupolar constant range is 10–80 MHz.[27,30,38]

Individual compounds

V_2O_5

The bonding geometry of V_2O_5 could be described as trigonal bipyramid (distorted six-coordinated) consisting of four equatorial V–O bonds of similar length with very short and very long axial V–O bonds. This coordination gives rise to a near axially symmetric chemical shift tensor. The structure of V_2O_5 is well-known and its ^{51}V NMR parameters have been reported numerously and verified by the structural

DOI: 10.1002/mrc

data from other methods. The ^{51}V NMR parameters obtained by SATRAS for V_2O_5[39] are given in Table 1. They are in good agreement with the data obtained for V_2O_5 monocrystal[40] and in addition confirmed by SATRAS calculations.[35]

Sc_2O_3

The structure of Sc_2O_3 contains two nonequivalent ScO_6 octahedra. The first one is an axially distorted octahedron with the Sc–O distances equal to 2.103 Å;[42] for the second octahedron four Sc–O distances equal 2.08 Å and the rest two equal 2.117 Å. The experimental static and MAS ^{45}Sc NMR spectra of Sc_2O_3 are shown in Fig. 2(1a) and (2a) These spectra result from a superposition of two lines indicating the presence of two nonequivalent sites. This is confirmed by line simulations, Fig. 2(1b–1d), and (2b–2d). Relative intensities of the simulated lines in Fig. 2(1c), (1d), and (2c), (2d) are close to 1 : 3, that agrees with the crystal structure.[42] The chemical shift anisotropy and quadrupolar constant of the axially symmetric site are reasonably large: $\delta_{CS} = 30$ ppm, $\eta_{CS} = 0.1$, $C_Q = 23.5$ MHz, $\eta_Q = 0.0$. The chemical shift anisotropy and quadrupolar constant of the distorted octahedron are rather small: $\delta_{CS} = 10$ ppm, $\eta_{CS} = 0.6$, $C_Q = 15.2$ MHz, $\eta_Q = 0.63$, Table 2. Recently, similar values were reported in Refs 18 and 21.

Nb_2O_5

Several Nb_2O_5 phases (Zeta, N, R, HT and M) are described in Refs 43, 44. A large number of nonequivalent Nb sites is a specific feature of all Nb_2O_5 phases. For instance, the HT phase has 15 nonequivalent Nb sites[43] contributing to the ^{93}Nb MAS and static NMR spectra. As a result the spectra are very wide. The line shapes are determined by large quadrupole coupling constant and moderate chemical shift anisotropy (the Nb–O distance varies from 1.753 to 2.478 Å in NbO_6): $C_Q = 18.0$ MHz, $\eta_Q = 1.0$, $\delta_{CS} = 290 \pm 10$ ppm,

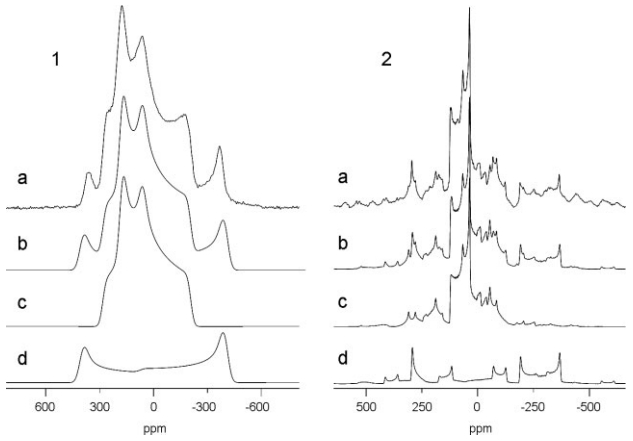

Figure 2. The static (1a) and central transition MAS (2a) ^{45}Sc NMR spectra of Sc_2O_3 obtained at magnetic field of 9.4 T and rotation frequency of 12 kHz; the static (1b–d) and central transition MAS (2b–d) simulation spectra of individual lines from Sc_1 (d), Sc_2 (c) and their superposition (b); the NMR parameters are given in Table 2.

$\eta_{CS} = 0.1 \pm 0.1$, $\delta_{iso} = -1175 \pm 10$ ppm with a Gaussian distribution of $C_Q \sim 5.5$ MHz. The isotropic chemical shift corresponds to six-coordinated Nb sites.[30] Various 'NbO_6' sites are hardly resolved in ^{93}Nb NMR spectra. According to Refs 30 and 38 even for rather different octahedral Nb sites ($Nb_2O_6^{2-}$, $Nb_2O_7^{4-}$, $Nb_4O_{13}^{6-}$, $Nb_4O_{15}^{10-}$, $Nb_2O_8^{6-}$) their C_Q and δ_{iso} hit narrow ranges: 14–22 MHz and −950 to 1110 ppm, respectively. Sufficient resolution could not be reached even in the experiments using ultimately high magnetic field (19 T) combined with ultra-fast sample rotation ($\nu_r > 35$ kHz). 19 T using rotation speed as high as 35 kHz did not lead to remarkable resolution in ^{93}Nb MAS NMR spectra of Nb_2O_5. The superposition of the lines, a broad distribution of the NMR parameters, is hardly analyzable.

Table 1. Parameters of ^{51}V quadrupole (C_Q, η_Q)[a] and chemical shift tensors (δ_{CS}, η_{CS}, δ_{iso})[b] for vanadates and solid solutions of REE obtained by analysis of 105.25 MHz ^{51}V static and MAS NMR spectra

Sample	x	V	C_Q (MHz)	η_Q	δ_{CS} (ppm)	η_{CS}	δ_{iso} (ppm)
$ScVO_4$		–	3.95 ± 0.01	0.01 ± 0.01	40 ± 5	0.83 ± 0.01	-674.9 ± 0.5
VNb_9O_{25}		–	3.95 ± 0.01	0.12 ± 0.01	100 ± 5	0.01 ± 0.01	-602.0 ± 0.5
VTa_9O_{25}		–	4.5 ± 0.05	0.1 ± 0.05	160 ± 5	0.06 ± 0.01	-617 ± 0.5
$NbVO_5$[41]		–	1.20 ± 0.05	0.39 ± 0.04	70 ± 4	0.17 ± 0.15	-791.4 ± 0.5
$TaVO_5$[41]		–	0.85 ± 0.02	0.28 ± 0.02	53 ± 4	0.24 ± 0.22	-773.2 ± 0.3
$VNb_{9(1-x)}Ta_{9x}O_{25}$		–	–	–	–	–	–
VNb_9O_{25}	0	V(4Nb)	4.00 ± 0.05	0.05 ± 0.02	100 ± 5	–	-601 ± 0.5
	2.7	V(3NbTa)	4.35 ± 0.05	0.01 ± 0.05	210 ± 10	0.06 ± 0.01	-607 ± 5
	4.5	V(2Nb2Ta)	4.38 ± 0.05	0.01 ± 0.05	210 ± 10	0.06 ± 0.01	-608 ± 5
	6.3	V(Nb3Ta)	4.5 ± 0.05	0.01 ± 0.05	160 ± 10	0.06 ± 0.01	-613 ± 5
VTa_9O_{25}	9.0	V(4Ta)	4.5 ± 0.05	0.1 ± 0.05	160 ± 5	0.06 ± 0.01	-617 ± 0.5
V_2O_5[39]	–	–	0.811 ± 0.01	0.04 ± 0.01	620 ± 5	0.15 ± 0.01	-609 ± 1

[a] Nuclear electric quadrupole moment eQ, electric field gradient tensor eigenvalues (V_1, V_2, and $V_3 = eq$) are expressed in terms of C_Q and η_Q: $C_Q = e^2qQ/h$; $V_1 = 1/2\,(-1 - \eta_Q)\,V_3$; $V_2 = 1/2\,(-1 + \eta_Q)V_3$.

[b] The eigenvalues of chemical shift tensor are expressed in terms of δ_{CS}, η_{CS} and δ_{iso}: $\delta_1 = -1/2\delta_{CS}\,(-1 - \eta_{CS}) + \delta_{iso}$, $\delta_2 = -1/2\delta_{CS}\,(-1 + \eta_{CS}) + \delta_{iso}$, $\delta_3 = -\delta_{CS} + \delta_{iso}$; δ_{iso} was determined from the simulation of the spectra and presented here with the second-order quadrupole shift correction.

DOI: 10.1002/mrc

Table 2. Parameters of ^{45}Sc quadrupole (C_Q, η_Q)[a] and chemical shift tensors (δ_{CS}, η_{CS}, δ_{iso})[b] for individual scandium compounds and solid solutions of REE obtained by analysis of 97.17 MHz ^{45}Sc static and MAS NMR spectra

Sample	x	C_Q (MHz)	η_Q	δ_{CS} (ppm)	δ_{iso} (ppm)	α	β	γ	ScO_n
$NaScO_2$[21]		14.2 ± 0.1	≤ 0.07	–	158.2 ± 0.4	–	–	–	ScO_6
$LiScO_2$[21]		1.6 ± 0.8	–	–	148.0 ± 0.6	–	–	–	ScO_6
Sc4[19]		15	0.6	–	127	–		–	ScO_6
Sc_2O_3		23.5 ± 0.1 (Sc1)	0.0 ± 0.01	30 ± 5	105 ± 5	–	–	–	ScO_6
		15.25 ± 0.1(Sc2)	0.63 ± 0.01	10 ± 5	126 ± 5	0	0	0	ScO_6
$Sc(TMHD)_3$[20]		13.1 ± 0.3	0.93	–	89.5 ± 1	0	15	90	ScO_6
$Sc(acac)_3$[20]		13.0 ± 0.3	0.22	–	82 ± 1	90	83	0	ScO_6
$ScNbO_4$		10.5 ± 0.1	1.0 ± 0.01	75 ± 5	93 ± 5	0	80	0	ScO_6
$ScTaO_4$		9.3 ± 0.1	1.0 ± 0.01	20 ± 5	83 ± 5	0	70	0	ScO_6
$ScNb_{(1-x)}Ta_xO_4$		–	–	–	–	–	–	–	–
$ScNbO_4$	0	10.5 ± 0.1	1.0 ± 0.01	75 ± 5	93 ± 5	0	80	0	ScO_6
	0.3	9.8 ± 0.1	1.0 ± 0.01	71 ± 5	96 ± 5	0	90	0	ScO_6
	0.5	9.7 ± 0.1	1.0 ± 0.01	45 ± 5	91 ± 5	0	70	0	ScO_6
	0.7	9.4 ± 0.1	1.0 ± 0.01	45 ± 5	80 ± 5	0	70	0	ScO_6
$ScTaO_4$	1.0	9.3 ± 0.1	1.0 ± 0.01	20 ± 5	83 ± 5	0	70	0	ScO_6
$Sc(OAc)_3$[20]		4.6 ± 0.2	0.18	–	-6.2 ± 1	0	7	90	ScO_6
$Sc(NO_3)_3\ 5H_2O$[20]		6.2 ± 0.2	0.75	–	-18.5 ± 1	80	10	65	ScO_8
$ScVO_4$		21.3 ± 0.1	0.0 ± 0.01	–	-30 ± 2	–	0	–	ScO_8
$ScVO_4$[21]		21.6 ± 0.1	≤ 0.03	–	-34 ± 0.5	–	–	–	ScO_8
$ScPO_4$[21]				–	-48.2	–	–	–	ScO_8

[a] Nuclear electric quadrupole moment eQ and electric field gradient tensor eigenvalues (V_1, V_2, and $V_3 = eq$) are expressed in terms of C_Q and η_Q: $C_Q = e^2qQ/h$; $V_1 = 1/2\ (-1 - \eta_Q)\ V_3$; $V_2 = 1/2\ (-1 + \eta_Q)\ V_3$.

[b] The eigenvalues of chemical shift tensor are expressed in terms of δ_{CS}, η_{CS} and δ_{iso}: $\delta_1 = -1/2\delta_{CS}\ (-1 - \eta_{CS}) + \delta_{iso}$, $\delta_2 = -1/2\delta_{CS}\ (-1 + \eta_{CS}) + \delta_{iso}$, $\delta_3 = -\delta_{CS} + \delta_{iso}$; δ_{iso} was determined from the simulation of the spectra and presented here with the second-order quadrupole shift correction.

VNb_9O_{25} and VTa_9O_{25}

VNb_9O_{25} and VTa_9O_{25} are isostructural compounds (tetragonal, space group I–4). The crystalline structure of three-dimensional VNb_9O_{25} is formed by a singular combination of two VO_4 tetrahedra and eighteen (Nb, Ta)O_6 octahedra per unit cell. The VO_4 tetrahedra are almost regular and all distances V–O are equal to 1.764 Å,[45] Fig. 3(a). The ^{51}V MAS NMR spectrum of VNb_9O_{25} is shown in Fig. 3(b). The line-shape is typical for low chemical shift anisotropy and moderate quadrupole coupling constant. The SATRAS parameters are present in Table 1. All features of the experimental spectrum in Fig. 3(b) are finely reproduced by the fit Fig. 3(c). The ^{51}V MAS NMR spectrum of VTa_9O_{25} is very similar to that of VNb_9O_{25}. The main characteristic of these spectra is the isotropic chemical shift: −602 and −617 ppm for VNb_9O_{25} and VTa_9O_{25}, respectively.

According to the structural data, there are three octahedral Nb sites with the following Nb–O distances: Nb_1–O varies from 1.909 (×2) to 1.981 Å (×4); Nb_2–O varies from 1.835 to 2.262 Å; Nb_3–O from 1.782 to 2.287 Å. The ratio of these sites is 2 : 8 : 8, respectively.[45] The ^{93}Nb NMR spectrum obtained at 9.4 T contains a narrow line from the most symmetric Nb_1 site and broad background from Nb_2 and Nb_3, Fig. 3(d). The later sites are characterized by a large quadrupole coupling constant and moderate chemical shift anisotropy. Even though it was hard to distinguish these sites based on the MAS spectrum, the isotropic shifts were estimated: −1180 ppm for Nb_2 and Nb_3; −1220 ppm for Nb_1. The upper limit of quadrupolar constant for Nb_1 is 20.0 MHz.

$NbVO_5$ and $TaVO_5$

$NbVO_5$ and $TaVO_5$ are isostructural compounds (orthorhombic, space group P_{nma}). The VO_4 tetrahedra share corners with (Nb, Ta)O_6 octahedra forming the pentagonal channels along the b-axis.[46] The ^{51}V NMR SATRAS parameters of these compounds (Table 1) are very similar and typical for Q^0 type.[41]

The quadrupolar part of the Hamiltonian dominates the ^{93}Nb NMR line-shape of the $NbVO_5$ spectrum (large quadrupole coupling constant, 16.5 MHz, and $\eta_Q = 0.9$).[47] Remarkably, the ^{93}Nb NMR spectrum of $NbVO_5$ is characterized by the largest isotropic chemical shift among all known Nb octahedral sites, $\delta_{iso} = -1338$ ppm.[30] This was referred to some peculiarities of the structure, when NbO_6 octahedra share corners.[47] However, structural features of this kind do not affect δ_{iso} as much as the covalence of the bonds.[30]

$ScVO_4$

$ScVO_4$ has a zircon type structure, $ZrSiO_4$, with a space group I–4_1/amd. In these structures equilateral VO_4 tetrahedra are slightly compressed along c-axis forming D_{2d} local symmetry. The ScO_8 structures are the slightly distorted dodecahedrons,[48] where four distances are equal to 2.129 Å, and the other four are 2.367 Å. The V–O distance is nearly

DOI: 10.1002/mrc

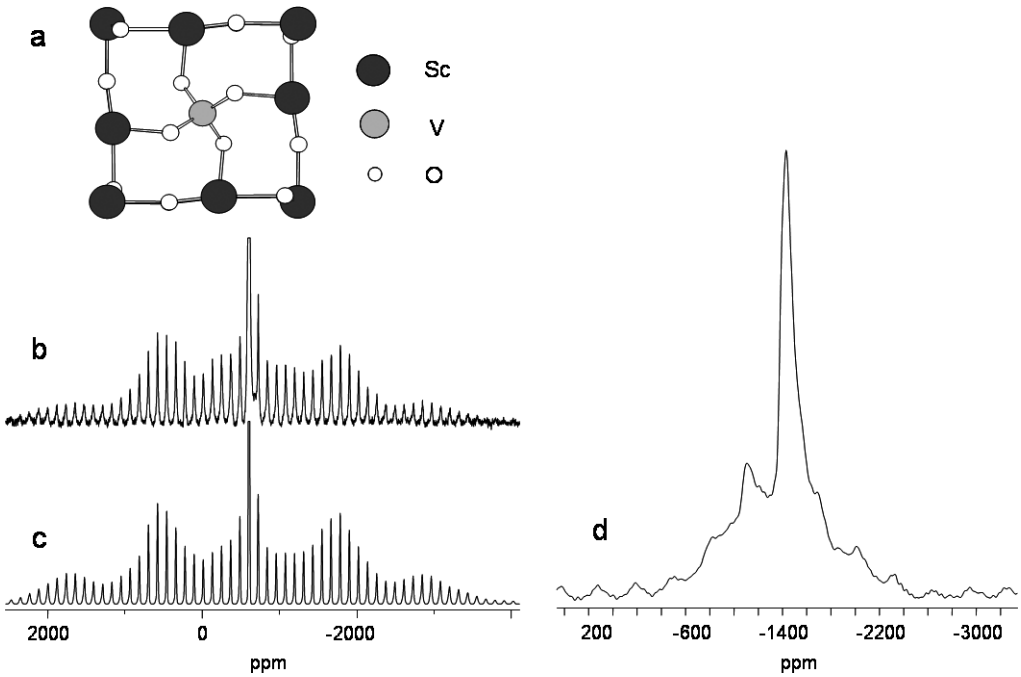

Figure 3. (a) The local structure of V sites in VNb_9O_{25}. (b) and (c) Experimental and simulated ^{51}V MAS NMR spectra of VNb_9O_{25} obtained at magnetic field of 9.4 T and rotation frequency of 12 kHz; the NMR parameters are given in Table 1. (d) The ^{93}Nb MAS NMR spectrum of VNb_9O_{25} recorded at 9.4 T and rotation frequency of 35 kHz.

the same in all Ln-vanadates and equal to 1.71–1.73 Å. An increase in Ln–O distance results in higher symmetry dodecahedron arrangement. The ^{51}V MAS NMR spectra of these compounds contain an intensive peak from the central transition and a set of spinning sidebands[49] characterized by low chemical shift anisotropy and moderate quadrupole coupling. All features of the experimental ^{51}V MAS NMR spectrum of $ScVO_4$ are finely reproduced by the fit, Fig. 4(2a) and (2b) The SATRAS parameters are listed in Table 1. The small chemical shift anisotropy is characteristic for isolated vanadium tetrahedra Q^0, and is typical for orthovanadates.

The static and MAS ^{45}Sc NMR spectra of $ScVO_4$ are shown in Fig. 4(3a), (3c), and (3e). The ^{45}Sc quadrupole coupling constant and chemical shift anisotropy are given in Table 2. On the basis of our ^{45}Sc MAS NMR data for Sc_2O_3 and $ScVO_4$, and using data from Refs 19–21 we propose the characteristic isotropic chemical shift ranges for polyhedrons ScO_6 and ScO_8 of Sc compounds, Table 2: for the coordination number 6 the chemical shift varies from 160 to −20 ppm; for coordination number 8 it ranges from −20 to −50 ppm.[18,19,21,37]

$ScNbO_4$ and $ScTaO_4$

$ScNbO_4$ and $ScTaO_4$ are isostructural compounds with the wolframite type structure ($FeWO_4$, monoclinic, space group *P12/C1*). In accordance with the structural data, both Sc and Nb (Ta) are present in octahedral oxygen environment with the distances close to those in $FeWO_4$: Fe–O (2.019 × 2, 2.081 × 2, 2.162 × 2 Å) and W–O (1.89 × 2, 2.00 × 2, 2.09 × 2 Å). The static and MAS ^{45}Sc NMR spectra of $ScNbO_4$ and $ScTaO_4$ are shown in Fig. 5, spectra a, e. These line-shapes result from large quadrupole coupling and small chemical shift anisotropy, Table 2. The parameters δ_{iso} of these spectra hit the range of the coordination number 6, Table 2. Owing to larger C_Q and lower field shift the symmetry of Sc environment seems to be lower for $ScNbO_4$ than for $ScTaO_4$, Table 2.

Solid solutions

$VNb_{9(1-x)}Ta_{9x}O_{25}$

A series of solid solutions $VNb_{9(1-x)}Ta_{9x}O_{25}$ ($x = 0$–1) exists in the range between VNb_9O_{25} and VTa_9O_{25}. All phases are crystalline and isostructural to VNb_9O_{25} (tetragonal, space group *I–4*).

^{51}V NMR is very sensitive to the second coordination sphere. Thus, the effects of Nb and Ta can be distinguished. The ^{51}V MAS NMR spectra of $VNb_{9(1-x)}Ta_{9x}O_{25}$ ($x = 0$, 0.3, 0.5, 0.7, 1) shown in Fig. 6 have similar features. Each spectrum consists of an almost isotropic line related to tetrahedral coordination of vanadium - Q^0, V_{tetr} (at *ca* from −607 to −613). For $x = 0$ and 1 the spectra correspond to VNb_9O_{25} and VTa_9O_{25}, respectively. The isolated VO_4 units of Q^0 type give rise to low chemical shift anisotropy, Table 1. For $x = 0.3$, 0.5 and 0.7 the broader lines are observed. The isotropic lines in the region from −600 to −620 ppm (vanadium in tetrahedral coordination Q^0) and their spinning sidebands are apparently a superposition of multiple components, Fig. 6(2). This reasonable guess, however, is difficult to confirm precisely due to the lack of resolution. In fact, several V sites are expected to form: V(4Nb), V(3NbTa), V(2Nb2Ta) *cis*- and *trans*-, V(Nb3Ta) and V(4Ta). The shifts of V(4Nb) and V(4Ta) are fixed, that simplifies the definition of the remaining three lines. For illustrative means, a suggestion for the line-shape decompositions is proposed in Fig. 6(2) (b), (c) and (d). As x increases, the isolated vanadium tetrahedra with four Nb

DOI: 10.1002/mrc

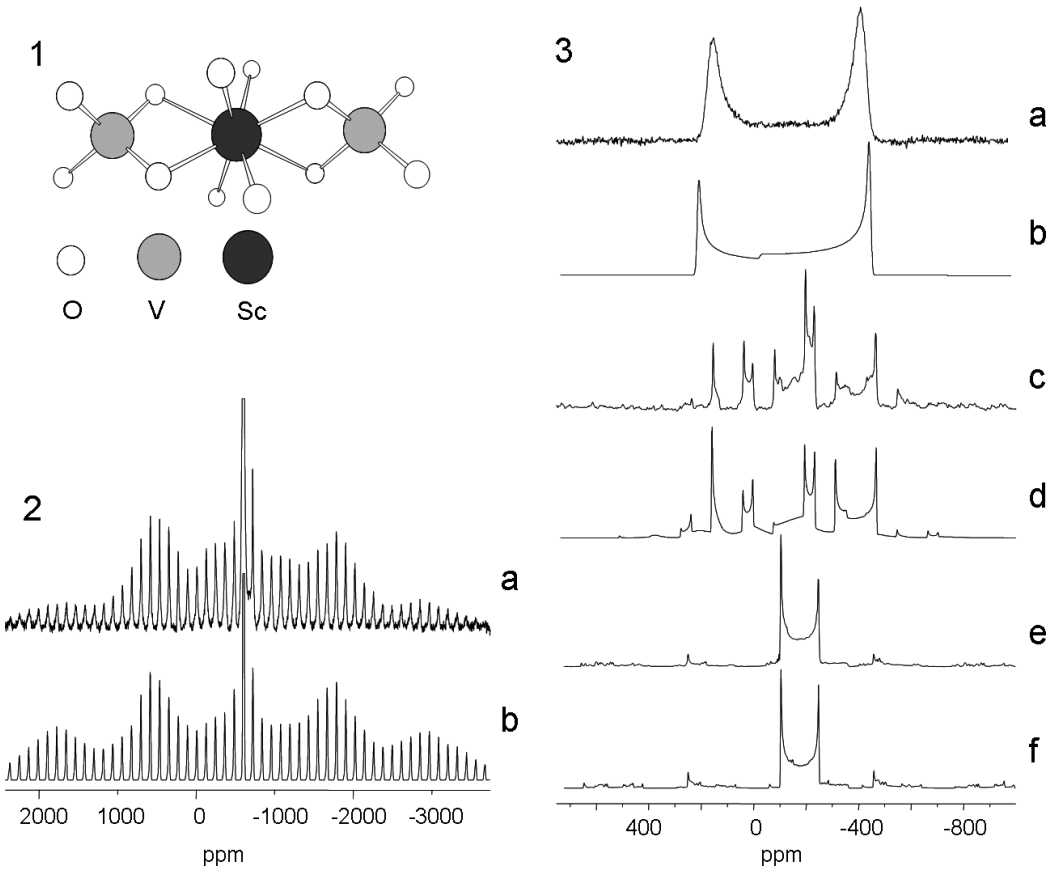

Figure 4. (1) Local structure of Sc and V sites in $ScVO_4$. (2) The experimental (a) and simulated (b) ^{51}V MAS NMR spectra of $ScVO_4$ obtained at magnetic field of 9.4 T and rotation frequency of 12 kHz. The NMR parameters are given in Table 1. (3) The experimental static (3a) and central transition MAS ^{45}Sc NMR spectra (3c and 3e) of $ScVO_4$ obtained at magnetic field of 9.4 T and rotation frequency of 12 kHz (c) and 35 kHz (e). (3b), (3d) and (3f) are the simulations of the spectra (3a), (3c) and (3e), respectively; the NMR parameters are given in Table 2.

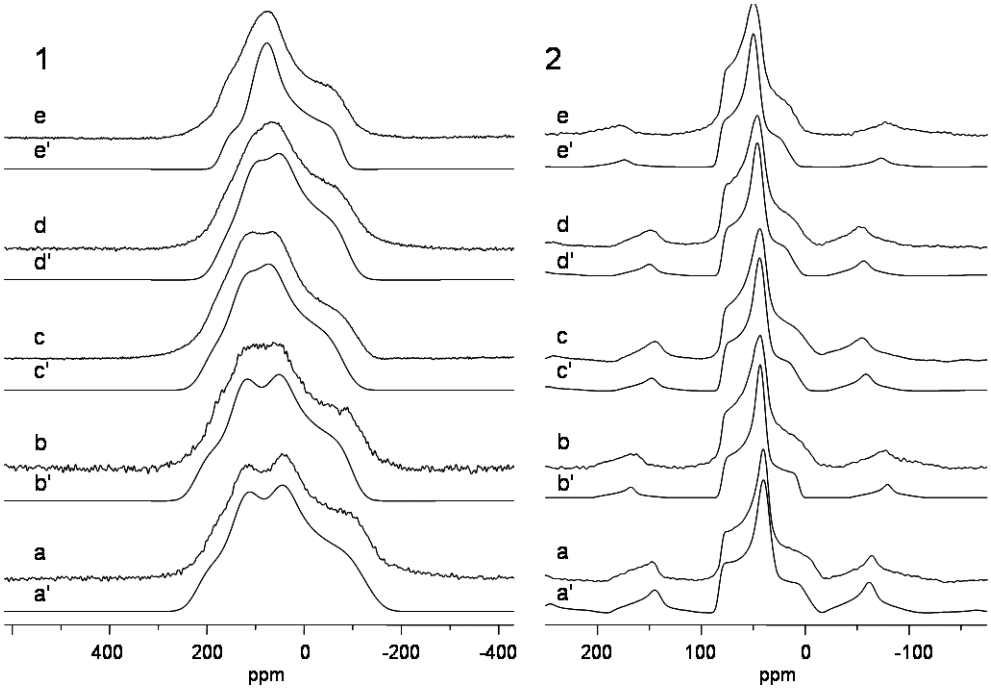

Figure 5. The experimental static (1) and MAS (2) ^{45}Sc NMR spectra of individual compounds $ScNbO_4$ (a) and $ScTaO_4$ (e), and solid solution $ScNb_{(1-x)}Ta_xO_4$: $x = 0.3$ (b), 0.5 (c) and 0.7 (d) obtained at magnetic field of 9.4 T and rotation frequency of 12 kHz; the simulation spectra are from (a′) to (e′), respectively.

DOI: 10.1002/mrc

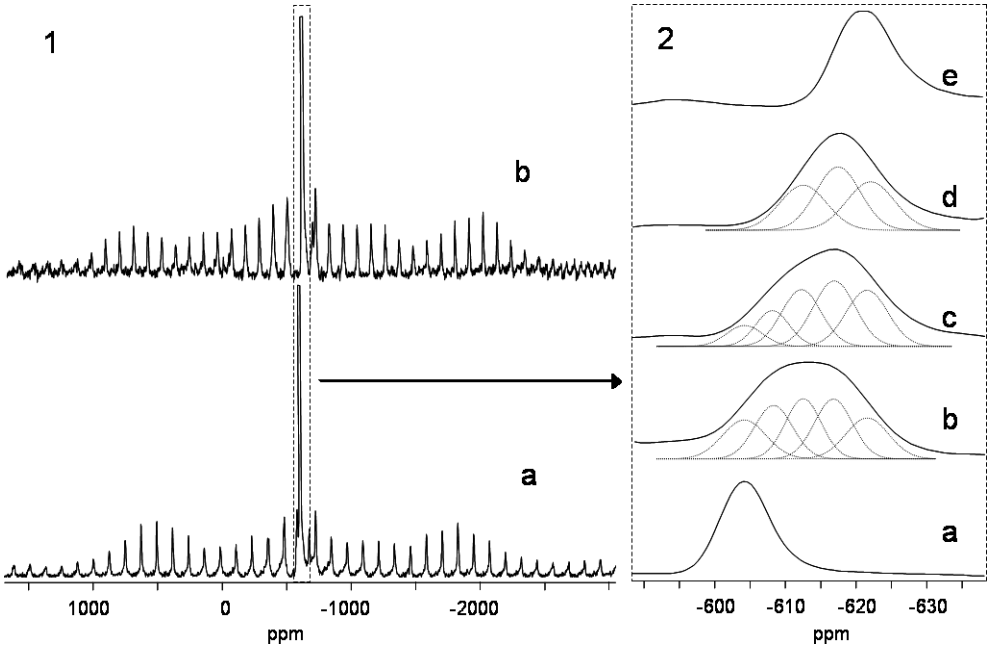

Figure 6. (1) The experimental ^{51}V MAS NMR spectra of $VNb_{9(1-x)}Ta_{9x}O_{25}$ for $x = 0.0$ (a) and 1.0 (b). (2) The isotropic shift region of the ^{51}V MAS NMR spectra for $x = 0.0$ (a), 0.3 (b), 0.5 (c), 0.7 (d) and 1.0 (e) – the decomposition is on the basis of the assumption of additively increasing chemical shift; the NMR parameters are given in Table 1.

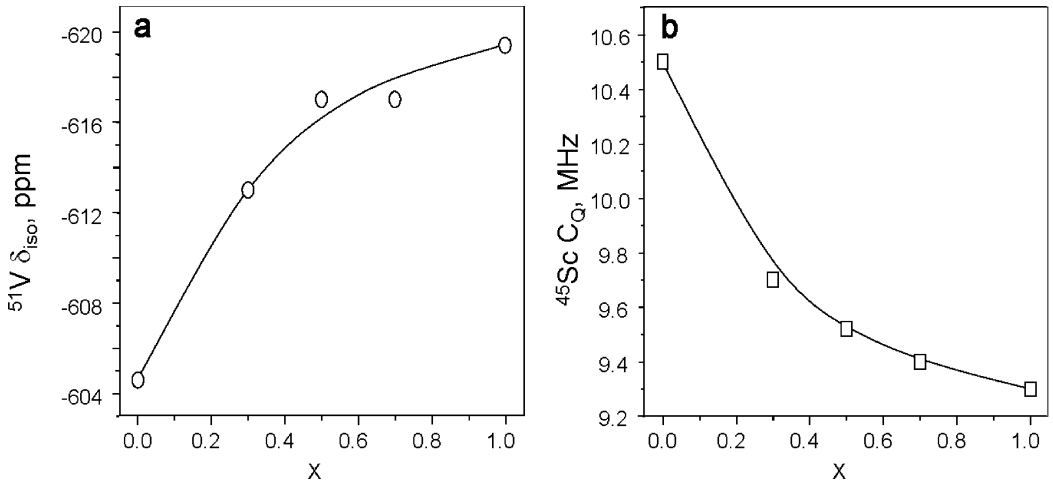

Figure 7. (a) The ^{51}V NMR isotropic chemical shifts, δ_{iso}, calculated for $VNb_{9(1-x)}Ta_{9x}O_{25}$ *versus* x. (b) The quadrupolar constants, C_Q, of ^{45}Sc calculated for $ScNb_{(1-x)}Ta_xO_4$ *versus* x.

atoms in the second coordination sphere are replaced by vanadium tetrahedra surrounded by 1, 2, 3 or 4 Ta atoms. The complete substitution of VNb_9O_{25} sites by that of VTa_9O_{25} gives rise to a single line of VTa_9O_{25}. The chemical shift, δ_{iso}, as a function of x is given in Fig. 7(a).

$ScNb_{(1-x)}Ta_xO_4$

Solid solutions of the series $ScNb_{(1-x)}Ta_xO_4$ ($x = 0$–1) have the wolframite structure, $FeWO_4$. The state of the cation sublattice was confirmed by ^{45}Sc NMR spectra. The static and MAS ^{45}Sc NMR spectra consisting of a single line are shown in Fig. 5. In agreement with the NMR of individual compounds, for $x = 0$ and 1 the observed lines correspond to the coordination number 6, Table 2. At increasing x from 0 to 1.0 δ_{iso} goes up field and C_Q decreases, Table 2, Figs 5 and 7(b). Thus, the environment of Sc seems to become more symmetric. The observed gradual change of NMR parameters, indeed, is typical for solid solutions.

$ScNb_{2(1-x)}Ta_{2x}VO_9$

The presence of three-dimensional solid solution based on VNb_9O_{25} was suggested for $ScNb_{2(1-x)}Ta_{2x}VO_9$.[5,10,50] The ranges of solid solution are determined by the following compounds: $TaNbV_2O_{10}$, $ScNb_2VO_9$, $ScTa_2VO_9$, VNb_9O_{25}, VTa_9O_{25}. All compounds in this range may be related with a formula: Me_4O_{10}: $TaNbV_2O_{10}$; or $Me_{20}O_{50}$: VNb_9O_{25}, VTa_9O_{25}; or Me_4O_9: $ScNb_2VO_9$, $ScTa_2VO_9$; or $Me_{20}O_{45}$, where $Me_4 = Ta + Nb + V_2 = Sc + Nb_2 + V = Sc + Ta_2 + V$; $Me_{20} = 5 \cdot (Ta + Nb + V_2) = 5 \cdot (Sc + Nb_2 + V) = 5 \cdot (Sc + Ta_2 + V) = 2 \cdot (V + Nb_9) = 2 \cdot (V + Ta_9)$. For compounds

DOI: 10.1002/mrc

$TaNbV_2O_{10}$–ScR_2VO_9 the replacement of Ta, Nb and V by Sc occurs via vacancy mechanism, i.e. compound $Me_{20}O_{50}$ is replaced by $Me_{20}O_{45}$. In addition, partial replacement of oxygen by Sc in $TaNbV_2O_{10}$ is followed by formation of oxygen vacancies, i.e. $Me_{20}O_{50}$ is replaced by $Me_{20}O_{45}$.

The replacement mechanism in VR_9O_{25}–ScR_2VO_9 is similar: Nb or Ta is partly replaced by Sc and V. It seems that in the full range of solid solution a quite complicated mechanism of replacement takes place. The real mechanism can be combined with those mentioned above. The similarity of the X-ray diffraction patterns of $TaNbV_2O_{10}$, $ScNb_2VO_9$, $ScTa_2VO_9$, VNb_9O_{25} and VTa_9O_{25} does not allow identification of either individual compounds or solid solutions in the primary mixture. The NMR as a nuclei-sensitive technique is the most efficient in this case. The ^{51}V NMR chemical shift sensitivity to the second coordination sphere allows identification of REE orthovanadates despite having almost an identical structure with the first coordination sphere. For instance, replacement of Nb by Ta ($VNb_9O_{25} \rightarrow VTa_9O_{25}$ and $NbVO_5 \rightarrow TaVO_5$) give rise to 20 ppm shift. The ^{51}V NMR spectra of $NbVO_5$ and $TaVO_5$ are essentially shifted to high field (190 ppm) with respect to that of VNb_9O_{25} and VTa_9O_{25}.

If the mechanism proposed in Ref. 50 is true, and the structures of $ScNb_2VO_9$ and VNb_9O_{25} are similar, the three extra V atoms of $ScNb_2VO_9$ should be located in octahedral sites of Nb, five Nb positions should be occupied by Sc atoms and a considerable change of Nb framework is expected. Without a doubt, ^{51}V NMR would be sensitive to this change of structure: additional lines corresponding to V octahedra must appear and the lines related to V tetrahedra should change respectively. For all series $ScNb_{2(1-x)}Ta_{2x}VO_9$ the lines related to the VNb_9O_{25} sites were apparent. In addition, minor lines related to V in a distorted tetragonal pyramid were present. A part of tetragonal pyramid vanadium determined for $ScNb_2VO_9$ and $ScTa_2VO_9$ did not exceed a few percent, that is not coherent with 60% contribution claimed in Ref. 50 The X-ray analysis performed for $ScNb_{2(1-x)}Ta_{2x}VO_9$ seems to be ambiguous, in contrast to NMR data. The fact that under air atmosphere the solid solutions of this series are very instable can explain inconsistency of NMR and X-ray results. Mixing of phases was also confirmed by NMR for $LaNb_{2(1x)}Ta_{2x}VO_9$ and $YNb_{2(1-x)}Ta_{2x}VO_9$.

CONCLUSION

Solid state ^{51}V, ^{45}Sc, and ^{93}Nb NMR allowed us to describe the structural composition of the complex solid mixtures: $VNb_{9(1-x)}Ta_{9x}O_{25}$, $ScNb_{1-x}Ta_xO_4$ and $ScNb_{2(1-x)}Ta_{2x}VO_9$ (x = 0, 0.3, 0.5, 0.7, 1.0). The gradual change of NMR parameters with x confirms $ScNb_{(1-x)}Ta_xO_4$ and $VNb_{9(1-x)}Ta_{9x}O_{25}$ to be solid solutions. These results are on the basis of the analysis of quadrupole coupling and chemical shift tensors obtained for a set of individual compounds by simulation of ^{51}V, ^{45}Sc, ^{93}Nb NMR spectra. The suggested ^{45}Sc chemical shift scaling for oxygen coordination number is applicable for the characterization of Sc–compounds by solid state NMR. To summarize, ^{93}Nb MAS NMR may appear ineffective even if ultimately high magnetic fields are used.

Acknowledgements

This work was supported by RFBR grant 07-03-00695-a. We are grateful to Professors A. A. Shubin and R. N. Pletnev, and Drs L.A. Perelyaeva and L.V. Zolotukhina for fruitful advice and preparation of the samples.

REFERENCES

1. Zuev MG, Zolotukhina LV. *Zh. Neorg. Khim.* 1990; **35**: 2185.
2. Zuev MG, Arhipova EV. *Russ. J. Inorg. Chem.* 1999; **44**: 1118.
3. Arkhipova EV, Zuev MG, Zolotukhina LV. *J. Alloys Compd.* 2000; **305**: 58.
4. Zuev MG. *Russ. Chem. Rev.* 2000; **69**: 551.
5. Zolotukhina LV, Zabolotskaya YeV, Arkhipova YeV, Zuev MG. *J. Phys. Chem. Solids* 2002; **63**: 415.
6. Banares MA, Wachs IE, Martin-Aranda RM (eds). *Group Five Compounds*, UNED: Toledo, 2002.
7. Wachs IE (ed). *Group Five Compounds*, Lehigh University: Jiminy Peak, Hancock, Massachusetts, 2005.
8. Zuev MG, Arkhipova EV, Perelyaeva LA, Zolotukhina LV, Lapina OB, Pletnev RN. *J. Solid State Chem.* 2002; **167**: 73.
9. Perelyaeva LA, Zolotukhina LV, Krystallov LV, Zabolotskaya YeV, Zuev MG, Arkhipova YeV. *Zh. Neorg. Mater.* 2000; **36**: 588.
10. Arkhipova EV, Zuev MG, Perelyaeva LA. *J. Alloys Compd.* 2006; **414**: 48.
11. Duer MJ. *Solid-state NMR Spectroscopy Principles and Applications*. Blackwell Science: Malden MA, UK, 2002.
12. Mastikhin VM, Lapina OB. In *Encyclopedia of Nuclear Magnetic Resonance*, vol. 8, Grant DM, Harris RK (eds). John Wiley & Sons: Chichester, 1996; 4892 (and references therein).
13. Lapina OB, Shubin AA, Khabibulin DF, Terskikh VV, Bodart PR, Amoureux JP. *Catal. Today* 2003; **78**: 91 (and references therein).
14. Thompson AR, Oldfield E. *J. Chem. Soc., Chem. Commun.* 1987; 27.
15. Pike KJ, Malde RP, Ashbrook SE, McManus J, Wimperis S. *Solid State Nucl. Magn. Reson.* 2000; **16**: 203.
16. Ashbrook SE, Wimperis S. *J. Magn. Reson.* 2002; **156**: 269.
17. Bräuniger T, Ramaswamy K, Madhu PK. *Chem. Phys. Lett.* 2004; **383**: 403.
18. Riou D, Fayon F, Massiot D. *Chem. Mater.* 2002; **14**(5): 2416.
19. Park HS, Bull I, Peng LM, Victor GYJ, Grey CP, Parise JB. *Chem. Mater.* 2004; **16**: 5350.
20. Rossini AJ, Schurko RW. *J. Am. Chem. Soc.* 2006; **128**: 10391.
21. Kim N, Hsieh CH, Stebbins JF. *Chem. Mater.* 2006; **18**: 3855.
22. Cotts RM, Knight WD. *Phys. Rev.* 1954; **96**: 1285.
23. Wolf F, Kline D, Story HS. *J. Chem. Phys.* 1970; **53**: 3538.
24. Man PP, Theveneau H, Papon P. *J. Magn. Reson.* 1985; **64**(2): 271.
25. Amoureux J-P. *Solid State Nucl. Magn. Reson.* 1993; **2**: 83.
26. Amoureux J-P, Fernandez Ch, Frydman L. *Chem. Phys. Lett.* 1996; **259**: 347.
27. Du LS, Schurko RW, Kim N, Grey CP. *J. Phys. Chem. A* 2002; **106**: 7876.
28. Prasad S, Zhao P, Huang J, Fitzgerald JJ, Shore JS. *Solid State Nucl. Magn. Reson.* 1999; **14**: 231.
29. Prasad S, Zhao P, Huang J, Fitzgerald JJ, Shore JS. *Solid State Nucl. Magn. Reson.* 2001; **19**: 45.
30. Lapina OB, Khabibulin DF, Romanenko KV, Gan Z, Zuev MG, Krasil'nikov VN, Fedorov VE. *Solid State Nucl. Magn. Reson.* 2005; **28**: 204.
31. Herzfeld J, Berger AE. *J. Chem. Phys.* 1980; **73**(12): 6021.
32. Skibsted J, Nielsen NC, Bildsøe H, Jakobsen HJ. *Chem. Phys. Lett.* 1992; **188**(5–6): 405.
33. Jaeger C. In *NMR Basic Principles and Progress*, Blumlich B, Kosfeld R (eds). Springer: Berlin, 1994; 133.
34. Shubin AA, Lapina OB, Zhidomirov GM. IX International AMPERE Summer School on magnetic resonance, Novosibirsk, 1987; 103.
35. Shubin AA, Lapina OB, Bosch E, Spengler J, Knözinger H. *J. Phys. Chem. B* 1999; **103**: 3138.

36. Shubin AA, Lapina OB, Bondareva VM. *Chem. Phys. Lett.* 1999; **302**: 341.
37. Mason J. *Multinuclear NMR*. Plenum Press: New York and London, 1987; 493.
38. Fitzgerald JJ, Prasad S, Huang J, Shore JS. *J. Am. Chem. Soc.* 2000; **122**: 2556.
39. Fernandez C, Bodart P, Amoureux JP. *Solid State Nucl. Magn. Reson.* 1994; **3**: 79.
40. Gornostansky SD, Stager GV. *J. Chem. Phys.* 1967; **46**: 4959.
41. Skibsted J, Jacobsen CJH, Jakobsen J. *Inorg. Chem.* 1998; **37**: 3083.
42. Bartos A, Lieb KP, Uhrmacher M, Wiarda D. *Acta Crystallogr., Sect. B* 1993; **49**: 165.
43. Kato K. *Acta Crystallogr., Sect. B* 1976; **32**: 764.
44. Ercit TS. *Mineral. Petrol.* 1991; **43**: 217.
45. Casais MT, Gutierrez-Puebla E, Monge MA, Rasines I, Ruiz-Valero C. *J. Solid State Chem.* 1993; **102**: 261.
46. Amarilla JM, Casal B, Ruiz-Hitzky E. *Mater. Lett.* 1989; **8**: 132.
47. Davis J, Tinet D, Fripiat JJ, Amarillo JM, Casal B, Ruiz-Hitzky E. *J. Mater. Res.* 1991; **6**(2): 393.
48. Fotiev AA, Slobodin BV, Khodos MYa. *Vanadates, Structure, Synthesis, Properties*. Nauka: Moscow, 1988.
49. Khabibulin DF, Shubin AA, Lapina OB. In *NATO ASI, Magnetic Resonance in Colloid and Interface Science*, vol. 76, Fraissard J, Lapina O (eds). Kluwer: The Netherlands, 2002; 537.
50. Arkhipova EV. *Phase Relations and Spectral Features of the New Compounds Formed in* $M_2O_3–V_2O_5–Ta_2O_5–Nb_2O_5$ *(M – Sc, Y, La) Systems*. Institute of Solid State Chemistry. PhD Thesis, Ekaterinburg, 2003; 147 (in Russian).

DOI: 10.1002/mrc